

Heavy hadrons on $N_f = 2$ and $2 + 1$ improved clover-Wilson lattices

Tommy Burch¹ *

¹*D-93053 Regensburg, Germany*

We present the masses of singly (B , B_s , Λ_b , Σ_b , etc.), doubly (B_c , η_b , Υ , Ξ_{bc} , Ξ_{bb} , etc.), and triply (Ω_{bcc} , Ω_{bbc} , Ω_{bbb} , etc.) heavy hadrons arising from (QCDSF-UKQCD) lattices with improved clover-Wilson light quarks. For the bottom quark, we use an $O(a, v^4)$ -improved version of lattice NRQCD. Part of the bottomonia spectrum is used to provide an alternative scale and to determine the physical quark mass and radiative corrections used in the heavy-quark action. Results for spin splittings, opposite parities, and, in some cases, excited states are presented. Higher lying states and baryons with two light quarks appear to be especially affected by the relatively small volumes of this (initially) initial study. This and other systematics are briefly discussed.

PACS numbers: 11.15.Ha, 12.38.Gc, 12.39.Hg, 14.20.Mr, 14.40.Nd

I. INTRODUCTION

Ditto the above [1].

Here are some references concerning experimental and lattice-QCD results for heavy-hadron spectroscopy:

New bottomonia, including the ground-state η_b [2–4] and the corresponding “radial” excitation $\eta_b(2S)$ [5, 6], the spin-singlet P -waves $h_b(1P)$ and $h_b(2P)$ [7], and a possible $\chi_b(3P)$ [8];

Orbitally excited B and B_s mesons [9–12];

$\Sigma_b^{(*)}$ [13], Ξ_b [14, 15], and Ω_b baryons [16–18]. Excited Ξ_b [19] and Λ_b baryons [20, 21];

Lattice studies of bottomonia [22–24], including those with charm sea-quarks [25, 26], and predictions of D -wave [27] and higher states [28];

Lattice results for B and B_s mesons [29–36], including predictions for the B_c system [37, 38];

Lattice results for b -baryons [31, 39, 40] and triply bottom baryons [41, 42].

Some more recent developments: Lattice studies of bc baryons [43], bottomonia [44], and positive parity B_s mesons [45]; and the experimentalists have been busy with the $\chi_b(3P)$ state and Ξ_b baryons [46–48].

For heavy-quark-model calculations, see, e.g., Ref. [49].

Once again [1].

II. LATTICE CALCULATION

In the present section we give the details of the simulations: the gauge configurations used, how the quark propagators are calculated, and how these are put together to form the correlators for the hadrons of interest.

A. Configurations

We use gauge configurations which include either $N_f = 2$ flavors of non-perturbatively improved clover-Wilson quarks [50] or $N_f = 2 + 1$ flavors of SLiNC quarks [51]. The relevant parameters of the ensembles used can be found in Table I. As can be seen in the last column, the spatial extent of the lattices is rather small. Whereas this may not strongly affect tightly bound, multiply heavy systems (e.g., Υ , B_c , Ω_{bcc} , etc.), higher excitations and hadrons with lighter valence quarks may “feel the pinch” [52] and this is therefore a source of systematic error which we must keep in mind.

B. Light and charm quark propagators

The propagators for the light (u, d), strange (s), and charm (c) quarks were produced using the Chroma software library [53]. The light-quark propagators on ensemble **a** and the light- and strange-quark propagators on ensembles **b** and **e** were originally created for other projects (see [50] and [54], respectively) and we must work with the (rather severe) quark-source smearings chosen therein (see Table II; of course, with great computational advantage of just having to read in the files). The light- and strange-quark propagators on ensembles **c** and **d** and the charm-quark propagators on ensembles **b–e** were created with the aim of better resolving excited states (less smearing, see Table II). The charm-quark mass was

TABLE I: Relevant lattice parameters [50, 51].

lbl	β	κ_{ud}, κ_s	$N_s^3 \times N_t$	N_{conf}	aM_π	$M_\pi L$
a	5.29	0.13632, –	$32^3 \times 64$	660	0.1070(5)	3.42
b	5.50	0.12104, 0.12062	$24^3 \times 48$	320	0.1406(8)	3.37
c	5.50	0.12100, 0.12070	$24^3 \times 48$	180	0.1515(10)	3.64
d	5.50	0.12095, 0.12080	$24^3 \times 48$	210	0.1661(8)	3.99
e	5.50	0.12090, 0.12090	$24^3 \times 48$	800	0.1779(6)	4.27

*tommy.burch@physik.uni-r.de

taken from a related study [54, 55] ($\kappa_c = 0.1109$). The lattice scale there, however, was set using a different observable (the flavor-singlet baryon-mass combination X_N [51]) than the one here ($M(1P) - M(1S)$ from $b\bar{b}$) and we therefore have a systematic shift in our B_c -system masses when using the bottomonia scale (see Sec. III B).

C. Non-relativistic quark propagators

For the bottom quark, we employ improved NRQCD [59], including terms up to $O(v^4)$, where v is the heavy-quark velocity. We use the time-step symmetric form of the evolution equation:

$$\begin{aligned} \phi(\mathbf{y}, t+a) &= \left(1 - \frac{a\delta H(t+a)}{2}\right) \left(1 - \frac{aH_0(t+a)}{2n}\right)^n \\ &\cdot U_4^\dagger(t) \left(1 - \frac{aH_0(t)}{2n}\right)^n \left(1 - \frac{a\delta H(t)}{2}\right) \\ &\cdot \phi(\mathbf{x}, t), \end{aligned} \quad (1)$$

where the binomial expression of the exponential of the lower-order (in v) terms is carried out to $n = 4$. H_0 handles the heavy-quark kinetic energy and the associated $O(a)$ time-step correction,

$$H_0 = -\frac{\tilde{\Delta}}{2m_Q} - \frac{a}{4n} \frac{\tilde{\Delta}^2}{4m_Q^2}, \quad (2)$$

and δH contains the $O(v^4)$ relativistic corrections,

$$\begin{aligned} \delta H &= -\frac{c_1}{8m_Q^3} \tilde{\Delta}^2 \\ &+ \frac{igc_2}{8m_Q^2} (\nabla \cdot \mathbf{E} - \mathbf{E} \cdot \nabla) \\ &- \frac{gc_3}{8m_Q^2} \sigma \cdot (\tilde{\nabla} \times \mathbf{E} - \mathbf{E} \times \tilde{\nabla}) \\ &- \frac{gc_4}{2m_Q} \sigma \cdot \mathbf{B}. \end{aligned} \quad (3)$$

TABLE II: Quark source smearings.

lbl	quark	sm.type	params.
a	u, d	Gauss [57] + APE [58]	$(\kappa = 0.25, N = 400) + (f = 2.5, N = 25)$
b	u, d, s	Gauss + APE	$(\kappa = 0.25, N = 150) + (f = 2, N = 20)$
c,d	u, d, s	Gauss + APE	$(\kappa = 0.25, N = 20) + (f = 2, N = 3)$
e	u, d, s	Gauss + APE	$(\kappa = 0.3, N = 130) + (f = 2, N = 20)$
b-e	c	Gauss + APE	$(\kappa = 0.25, N = 12) + (f = 2, N = 3)$
a-e	Q	Gauss	$(\kappa = 0.2, N = 16)$

Covariant derivatives and Laplacians with a tilde represent improved versions, where next-to-nearest neighbor sites are included (this is the same form of corrections we used in previous studies of bottomonia [60]; the form of the heavy-quark evolution, Eq. (1), has been improved for the present study [61]). The (chromo) electric and magnetic fields are constructed using the standard four-plaquette clover formalism (see, e.g., Ref. [62]) and tadpole improvement [59, 63] is applied throughout: $U_\mu(x) \rightarrow U_\mu(x)/u_0$, $\mathbf{E}(x) \rightarrow \mathbf{E}(x)/u_0^4$, $\mathbf{B}(x) \rightarrow \mathbf{B}(x)/u_0^4$, where u_0 is determined from the average plaquette. On each ensemble we run two or three different heavy-quark masses ($am_Q = 1.5 - 3.0$) and for the radiative corrections, we use tree-level values $c_i = 1$, as well as the case where $c_4 = 1.2$.

D. Hadron correlators

As already mentioned above (Table II), we use a combination of source smearings for all quark propagators. For the heavy quark (Q), we use the smeared source, as well as another where a covariant Laplacian is also applied (giving a radial node; for P - and D -wave mesons, we use a local source as the second choice). For all quarks we use local sinks, while for the heavy quark we also consider the two smearings used at the source. This leads to a rather peculiar situation where the heavy-quarkonia and triply-heavy-baryon correlators form 2×3 matrices, with a 2×2 symmetric block, whereas all correlators involving light, strange, or charm quarks, together with heavy ones, form 2×3 off-diagonal blocks of a larger (mostly unknown) matrix. This is not a major problem, however, as we can still fit such heavy-light correlators to the usual ansatz,

$$\begin{aligned} C(t)_{ij} &= \langle 0 | O_i(t) O_j^\dagger(0) | 0 \rangle \\ &= \sum_{n=1}^{\infty} v_i^{(n)} v_j^{(n)*} e^{-tE^{(n)}}, \end{aligned} \quad (4)$$

except that we must fix one amplitude for each energy level considered (the fit then gives amplitude ratios, but the same energies). For some fits, we find it advantageous to consider a submatrix (2×2 or 2×1) of the ones we have (this is likely due to limited statistics) and for most mass differences reported, we use appropriate (jackknifed) combinations of only the smeared-source, smeared-sink correlators (see below).

The interpolating operators that we use to combine the quarks together into the mesons of interest are shown in Tables III and IV. One needs to be careful when combining the u, d, s, c quark propagators from Chroma with the nonrelativistic Q propagators: a change in the spin-basis is needed [64].

The baryon operators can be found in Table V. In order to project out the desired spin and parity, the baryon

correlators should then be of the form

$$B^{1/2^\pm}(t) = \left\langle \frac{1}{2}(1 \pm \gamma_4) O \bar{O} \right\rangle \quad (5)$$

or, for operators with an open Lorentz index,

$$B_{ij}^{J^\pm}(t) = \left\langle \frac{1}{2}(1 \pm \gamma_4) P_{ik}^J O_k \bar{O}_j \right\rangle, \quad (6)$$

where the zero-momentum spin-projectors are $P_{ik}^{3/2} = \delta_{ik} - \frac{1}{3}\gamma_i\gamma_k$ and $P_{ik}^{1/2} = \frac{1}{3}\gamma_i\gamma_k$. In the end, we average over the nine remaining spatial indices (i, j). For the flavor projections, we follow lowest-order HQET and do not consider mixings between the different heavy-quark configurations (e.g., between Λ_Q and Λ_Q^2 in Table V; we mostly consider the heavy-light diquark configurations in order to reach the negative-parity states). Although it is a poorer approximation, we do the same when considering different charm-quark configurations (q or $q' = c$). Depending on the desired state, however, it may be that one must take care with the appropriate flavor projections of the light quarks ($q, q' = u, d, s$) [65].

We also create non-zero-momentum correlators (smeared source / local sink only; $\vec{p} = 2\pi\vec{n}/L$, where

TABLE III: Quarkonia operators.

lowest state	J_{min}^{PC}	irrep Λ	operator
η_b	0^{-+}	A_1	$\chi^\dagger \phi$
Υ	1^{--}	T_1	$\chi^\dagger \sigma_i \phi$
χ_{b0}	0^{++}	A_1	$\chi^\dagger \sum_i \sigma_i \nabla_i \phi$
χ_{b1}	1^{++}	T_1	$\chi^\dagger \sum_{jk} \epsilon_{ijk} \sigma_j \nabla_k \phi$
χ_{b2}	2^{++}	T_2, E	$\chi^\dagger (\sigma_i \nabla_j + \sigma_j \nabla_i - \frac{2}{3} \delta_{ij} \sum_k \sigma_k \nabla_k) \phi$
h_b	1^{+-}	T_1	$\chi^\dagger \nabla_i \phi$
η_{b2}	2^{-+}	E	$\chi^\dagger (\nabla_i \nabla_i - \nabla_j \nabla_j) \phi$
Υ_2	2^{--}	E	$\chi^\dagger (\nabla_i \nabla_j \sigma_k + \nabla_j \nabla_k \sigma_i) \phi$

TABLE IV: Heavy-light meson operators (for the relativistic quark: $q = \binom{u}{l}$) [64].

lowest state	J_{min}^P	irrep Λ	operator
B_q	0^-	A_1	$\chi^\dagger u$
B_q^*	1^-	T_1	$\chi^\dagger \sigma_i u$
B_{q0}^*	0^+	A_1	$\chi^\dagger l$
B_{q1}^*	1^+	T_1	$\chi^\dagger \sigma_i l$

TABLE V: Heavy baryon operators (for the NR quark: $Q = \binom{\phi}{0}$) [64].

label	states	J_{min}^P	s_{dq}	operator
Λ_Q	$\Lambda_b, \Xi_{bc}, \Omega_{bc}$	$\frac{1}{2}^+$	0	$(qC\gamma_5 q')Q$
Λ_Q^2	$\Lambda_b^{(*)}, \Xi_{bc}^{('', '*)}, \Omega_{bc}^{('', '*)}$	$\frac{1}{2}^\pm$	0	$(qC\gamma_5 Q)q'$
Σ_{Qi}	$\Sigma_b^{(*)}, \Xi_b^{('', '*)}, \Omega_b^{(*)}, \Xi_{bc}^{('', '*)}, \Omega_{bcc}^{(*)}, \dots$	$\frac{1}{2}^+, \frac{3}{2}^+$	1	$(qC\gamma_i q')Q$
Σ_{Qi}^2	$\Sigma_b^{(*, '*)}, \Xi_b^{('', '*), (*, '*)}, \Omega_b^{(*, '*)}, \dots$	$\frac{1}{2}^\pm, \frac{3}{2}^\pm$	1	$(qC\gamma_i Q)q'$
Ξ_{QQi}	$\Xi_{bb}^{(*, '*), (*, '*), (*, '*), \dots}$	$\frac{1}{2}^\pm, \frac{3}{2}^\pm$	1	$(QC\gamma_i Q)q$
Ω_{QQQi}	Ω_{bbb}	$\frac{3}{2}^+$	1	$(QC\gamma_i Q)Q$

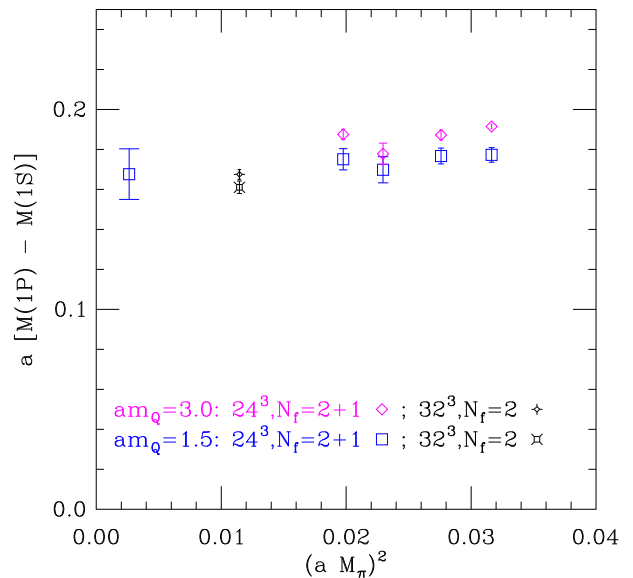


FIG. 1: Spin-averaged $1P - 1S$ $Q\bar{Q}$ mass differences versus pion mass.

$|\vec{n}| \leq 3$) for the Υ , B^* , and B_s^* in order to determine the kinetic masses of these mesons from their dispersion relations. This provides us with an absolute mass scale and a way to set (or interpolate to) the physical b -quark mass.

For many of the heavy baryons considered herein, we present an alternative analysis in which we try remove most of the remaining, leading uncertainties in the heavy-quark parameters. By considering appropriate combinations of (jackknifed) average correlators, we subtract $E(\Upsilon)/2$ for each b quark and $E(B_c) - E(\Upsilon)/2$ for each c quark. Inserting experimental values for $M(\Upsilon)$ and $M(B_c)$ into these mass differences, we arrive at more precise, absolute estimates of the heavy baryon masses, albeit via “less predictive” means.

III. ANALYSIS

In the following subsections we present our analysis of the heavy hadron correlators, leading to our results for the associated masses [66].

A. Quarkonia

At the present stage in this project we have not yet achieved a high-precision analysis of the bottomonia system; more precise studies may be found in Refs. [22–28]. However, we need to start somewhere and, as such, we are interested in using part of the $b\bar{b}$ spectrum to set the lattice scale and the parameters used in the heavy-quark action (m_Q, c_i). We present a few other results (spin splittings and excitations) along the way. Further

quarkonia simulations (e.g., on higher-statistics, larger-volume $N_f = 2 + 1$ ensembles), hopefully leading to a more complete analysis, are currently underway [1].

For spin-averaged and spin-dependent splittings we use single-elimination jackknife to create appropriate combinations (e.g., ratios or ratios of products) of the smeared-source, smeared-sink correlators to extract the ground-state energy differences and to handle the associated error correlations. One such example is the spin-averaged $1P - 1S$ mass difference:

$$\Delta M_{PS} = [5E(\chi_{b2}) + 3E(\chi_{b1}) + E(\chi_{b0})]/9 - [3E(\Upsilon) + E(\eta_b)]/4. \quad (7)$$

It is this quantity which we use to set the scale for the lattices. Figure 1 displays the results versus the pion mass. The leftmost point is the chirally extrapolated 24^3 , $N_f = 2 + 1$ difference (for $am_Q = 1.5 \approx am_b$, see below) and the closest black point is that for the 32^3 , $N_f = 2$ ensemble (a). Using the $b\bar{b}$ experimental value of 457 MeV [67], leads to $a^{-1} = 2726(206)$ MeV and 2837(55) MeV, respectively. Results from twice the heavy-quark mass ($am_Q = 3.0$) are also displayed, showing the relatively small dependence of this splitting on m_Q .

Using ground-state energy levels from the finite-momentum $Q\bar{Q}$ vector correlators, we fit the dispersion relation to the following form:

$$E = E_0 + \frac{p^2}{2M_{kin}} - \frac{p^4}{8M_{kin}^3}. \quad (8)$$

Resulting values for M_{kin} (in units of the $1P - 1S$ splitting, ΔM_{PS}) as a function of the pion mass are presented in Fig. 2. The larger error bars on the chirally extrapolated 24^3 result and on the 32^3 result are those which also include the error in the lattice spacing determination (about 7.5% and 2%, respectively; the same applies to all following figures). The experimental value of $M_T/\Delta M_{PS}$ is also plotted and one can see agreement when $am_Q = 1.5$ on the 24^3 , $N_f = 2 + 1$ lattices. For the 32^3 , $N_f = 2$ lattice, a slightly lower value for the heavy-quark mass ($am_Q \approx 1.3$) may have been appropriate. With the lack of a chiral extrapolation and the quenching of the strange quark, however, it is difficult to determine which systematics would become absorbed into such an adjustment. We use $am_Q = 1.5$ as our “working value” of the physical bottom-quark mass on all ensembles.

In order to find the radiative corrections for the spin-dependent terms (c_3 and c_4) in the heavy-quark action, we look at the “spin-orbit” and “tensor” energies of the $1P \ b\bar{b}$ system:

$$E_{SO} = [-2E(\chi_{b0}) - 3E(\chi_{b1}) + 5E(\chi_{b2})]/9, \quad (9)$$

$$E_T = [-2E(\chi_{b0}) + 3E(\chi_{b1}) - E(\chi_{b2})]/9. \quad (10)$$

These are roughly proportional to c_3 and c_4^2 , respectively (the corresponding experimental values are 18.20 MeV

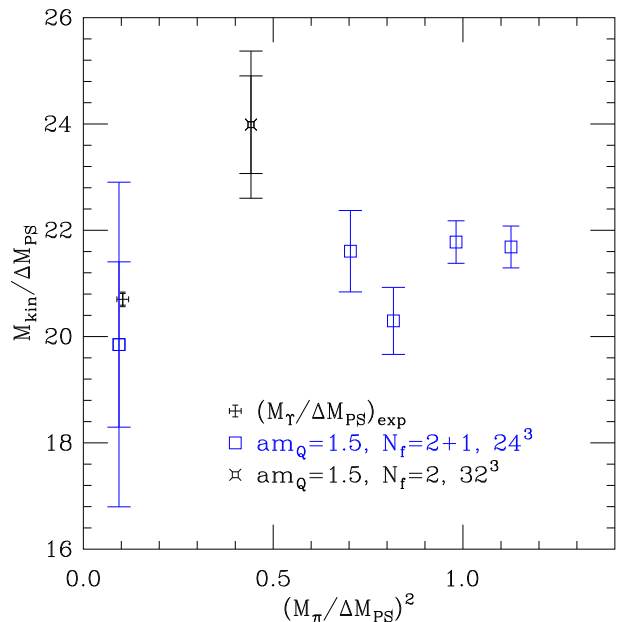


FIG. 2: Ground-state vector $Q\bar{Q}$ kinetic mass versus pion mass.

and 5.25 MeV). In Fig. 3, we plot our values for these energies for the cases where $c_3 = c_4 = 1$ and $c_3 = 1$, $c_4 = 1.2$. Within the errors the tree-level $c_3 = 1$ appears to work fine for E_{SO} , whereas the correction $c_4 = 1.2$ leads to better agreement for E_T . For the $N_f = 2$ results, a slightly higher c_4 appears to be needed (at least without a chiral extrapolation); together with a lower value for heavy-quark mass ($am_Q = 1.3$ for better M_{kin} and E_{SO} as well), the value $c_4 = 1.23$ would bring the tensor energy in better agreement with experiment. Now that the lattice scale and parameters of the heavy-quark action have been handled, we can turn our attention to other results.

Another quantity which follows from a jackknife ratio analysis is the spin splitting in the ground-state $b\bar{b}$ S -waves: $M(\Upsilon) - M(\eta_b)$. In Fig. 4 one can see that the 24^3 , $N_f = 2 + 1$ results extrapolate to a value slightly below the experimental value. However, when we include the error in the lattice spacing, we see that this discrepancy is only a little more than 1σ . The $N_f = 2$ result is also low, even after naively extrapolating to $am_Q = 1.3$, $c_4 = 1.23$ (using the $am_Q = 3.0$ and $c_4 = 1$ results).

We also use jackknife ratios to look more closely at the $1P$ spin splittings, including the h_b , and the energy differences to (and among) the $1D$ states. These results for the 24^3 , $N_f = 2 + 1$ chiral extrapolation, the $N_f = 2 + 1$ ensemble closest to the chiral limit (b), and the 32^3 , $N_f = 2$ ensemble (a) can be found in Table VI.

As eluded to earlier, we also fit the heavy-quarkonia correlator matrices to the form of Eq. (4). Depending upon the quantum numbers and time interval being considered, we fit anywhere from one to three energy levels.

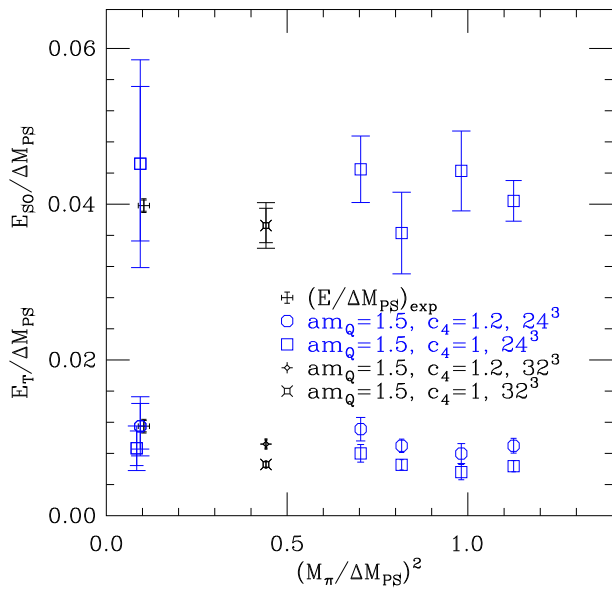


FIG. 3: Spin-orbit (SO) and tensor (T) energies from $1P$ $Q\bar{Q}$ states versus pion mass, showing that $c_3 = 1$, $c_4 = 1.2$ works best.

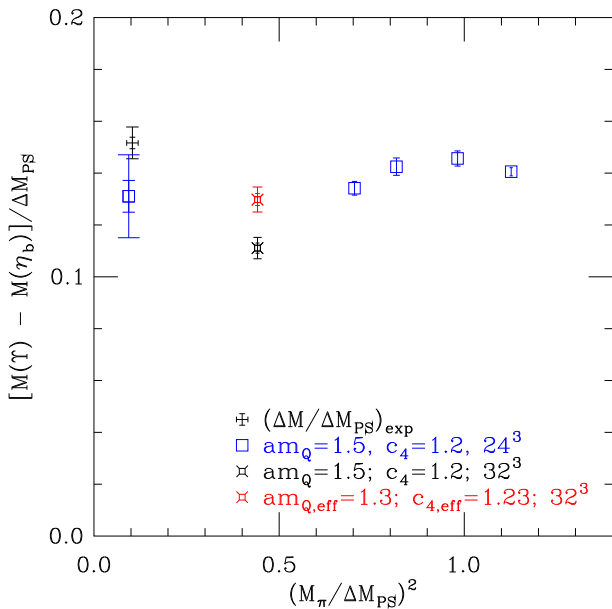


FIG. 4: $\Upsilon - \eta_b$ mass differences versus pion mass.

This provides us with estimates of the masses of first-excited states. The $N_f = 2$ and the chirally extrapolated $N_f = 2 + 1$ results are compiled in Table VI. One must be careful in interpreting the results of such states. The continuum-spin identification in Table III is the minimum possible (J_{min}) for the associated irreducible representation. Ideally, one should create the states of interest with operators in different lattice representations and look at the amplitudes as a way to confirm the associated spin

(see, e.g., [28, 68]). For the A_1 operators, after 0, the next lowest possible continuum spin is 4. Such states should be much higher in mass and we believe that we can say with confidence that the first-excited states we see for such operators are still spin 0. For the other representations, the separation in possible J values is not so large: the next lowest values are 3 for T_1 and T_2 and 4 for E . Luckily, for the case of the T_2 operator we have the E irreducible representation as well and can verify that the first excitation is consistent for both cases (in the end we average them). Otherwise, since the possible continuum-spin separation for the other operators is at least 2 and we are only dealing with first-excited states, we assume that $J = J_{min}$ for these states as well.

B. B , B_s , B_c mesons

Just as in the bottomonia case, we create jackknifed ratios of smeared-source, smeared-sink correlators to look at ground-state mass splittings of B mesons. Table VII shows the results for the $N_f = 2 + 1$ chiral limit, the $N_f = 2 + 1$ ensemble closest to the chiral limit (**b**), and the $N_f = 2$ ensemble (**a**).

The spin splittings for the S- and P-wave B mesons are shown in Figs. 5 and 6 as a function of the pion mass.

On all ensembles, the $B^* - B$ difference agrees with experiment. Replacing the light quark with a strange or charm one leads to our results for B_s and B_c mesons. $N_f = 2 + 1$ ground-state splittings, as well as differences to some first-excited states are shown in Table VIII. One may note the fact that the $B^* - B$ splitting appears to be slightly larger than that for $B_s^* - B_s$. This may be a sign of the small volumes' effect on the light quarks.

TABLE VI: Results for bottomonia mass splittings (in MeV) using $am_Q = 1.5$ and $c_4 = 1.2$ for the $N_f = 2 + 1$ chiral limit (χ), $N_f = 2 + 1$ ensemble **b**, and the $N_f = 2$ ensemble **a**. The first error comes from the fit, the second from the scale setting (ΔM_{PS}).

splitting	$N_f = 2 + 1$ (χ)	$N_f = 2 + 1$ (b)	$N_f = 2$ (a)
$\Upsilon - \eta_b$	59.7(2.8)(4.5)	58.7(1.1)(1.8)	50.76(90)(98)
$1P - \chi_{b0}$	46.8(7.5)(3.5)	43.9(3.1)(1.3)	32.9(1.5)(0.6)
$1P - \chi_{b1}$	10.4(4.4)(0.8)	9.4(1.8)(0.3)	9.04(86)(18)
$\chi_{b2} - 1P$	15.4(4.0)(1.2)	14.4(1.6)(0.4)	12.01(78)(23)
$1P - h_b$	1.3(1.8)(0.1)	2.13(64)(6)	1.09(50)(2)
$\eta_{b2} - 1S$	670(150)(50)	751(58)(23)	788(35)(15)
$\Upsilon_{b2} - 1S$	720(190)(55)	718(77)(22)	824(47)(16)
$\Upsilon_{b2} - \eta_{b2}$	130(95)(10)	60(40)(5)	21(18)(1)
$\eta'_b - \eta_b$	676(95)(51)	596(31)(18)	485(36)(9)
$\Upsilon' - \Upsilon$	671(97)(51)	584(33)(18)	474(38)(9)
$\chi'_{b0} - \chi_{b0}$	560(190)(40)	625(69)(19)	668(93)(13)
$\chi'_{b1} - \chi_{b1}$	690(200)(50)	684(76)(21)	729(97)(14)
$\chi'_{b2} - \chi_{b2}$	510(220)(40)	583(86)(18)	647(78)(13)
$h'_b - h_b$	620(200)(50)	630(79)(19)	654(79)(13)
$\eta'_{b2} - \eta_{b2}$	590(350)(45)	810(170)(30)	903(66)(18)
$\Upsilon'_{b2} - \Upsilon_{b2}$	1550(400)(120)	1170(140)(40)	990(190)(20)

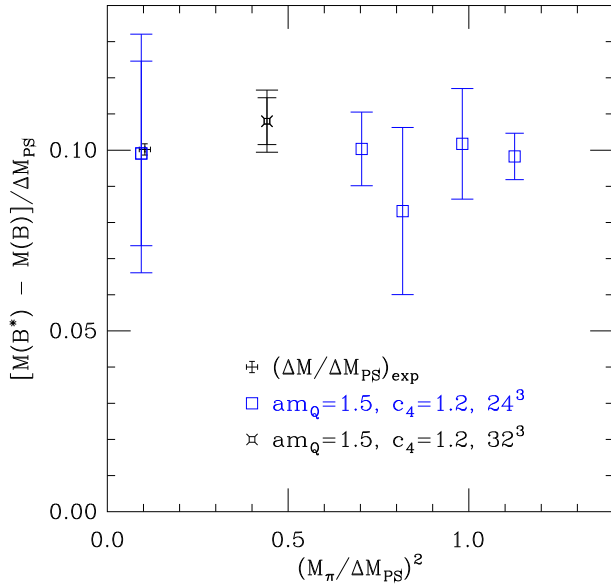
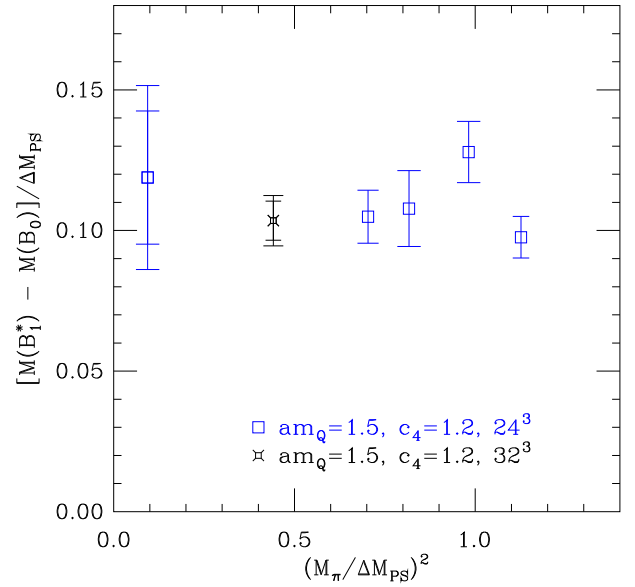
FIG. 5: $B^* - B$ mass differences versus pion mass.FIG. 6: $B_1^* - B_0^*$ mass differences versus pion mass.

Figure 7 displays the $B_{s_0}^* - B$ mass difference as a func-

TABLE VII: Results for B -meson mass splittings (in MeV) using $am_Q = 1.5$ and $c_4 = 1.2$ for the $N_f = 2 + 1$ chiral limit (χ), $N_f = 2 + 1$ ensemble **b**, and the $N_f = 2$ ensemble **a**. The first error comes from the fit, the second from the scale setting (ΔM_{PS}).

splitting	$N_f = 2 + 1$ (χ)	$N_f = 2 + 1$ (b)	$N_f = 2$ (a)
$B^* - B$	45(12)(3)	43.9(4.5)(1.3)	49.4(3.0)(1.0)
$B_1^* - B_0^*$	54(11)(4)	46.2(4.1)(1.4)	47.3(3.2)(0.9)
$B_0^* - B$	281(47)(21)	265(25)(8)	357(29)(7)
$B_1^* - B^*$	253(46)(19)	256(25)(8)	357(29)(7)

TABLE VIII: Results for $B_{(s,c)}$ -meson mass splittings (in MeV) using $am_Q = 1.5$ and $c_4 = 1.2$. for the $N_f = 2 + 1$ chiral limit (χ) and $N_f = 2 + 1$ ensemble **b**. The first error comes from the fit, the second from the scale setting (ΔM_{PS}).

splitting	$N_f = 2 + 1$ (χ)	$N_f = 2 + 1$ (b)
$B_s^* - B_s$	43(10)(3)	42.7(3.8)(1.3)
$B_{s1}^* - B_{s0}^*$	49.4(9.4)(3.7)	45.4(3.4)(1.4)
$B_s^* - B^*$	81(21)(6)	30.9(3.1)(0.9)
$B_{s0}^* - B$	418(29)(32)	345(12)(10)
$B_{s1}^* - B^*$	396(29)(30)	332(13)(10)
$B_c^* - B_c$	52.0(4.5)(3.9)	55.4(1.4)(1.7)
$B_{c1}^* - B_{c0}^*$	46(20)(3)	56.5(6.5)(1.7)
$B_c^* - B^*$	1165(79)(88)	1119(28)(34)
$B_{c0}^* - B$	1405(79)(106)	1417(31)(43)
$B_{c1}^* - B^*$	1346(82)(102)	1404(31)(43)
$B_{c'} - B_c$	560(260)(40)	780(120)(25)
$B_{c'}^* - B_c^*$	600(250)(45)	780(100)(25)
$B_{c0}^* - B_{c0}^*$	460(360)(35)	750(120)(25)
$B_{c1}^* - B_{c1}^*$	460(310)(35)	796(120)(25)

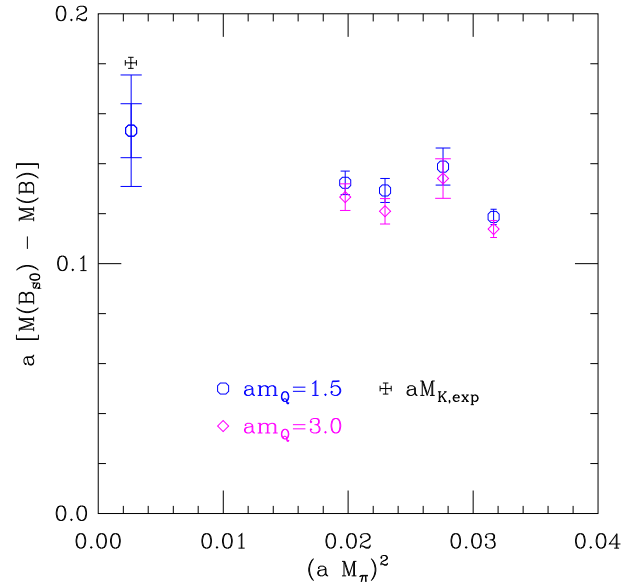


FIG. 7: $B_{s_0}^* - B$ mass differences versus pion mass. Indications are that the $B_{s_0}^*$ is below the BK threshold.

tion of pion (and thereby the kaon) mass. All indications are that the $B_{s_0}^*$ is below the BK threshold. The same is true for the B_{s1}^* and the B^*K threshold (see Table VIII).

Due to the rather large amount of smearing used for the light- and strange-quark sources on ensembles **b** and **e** [54] (see also Table II), we are not able to resolve radially excited $B^{(*)}$ or $B_s^{(*)}$ mesons on these ensembles (and therefore, not in the chiral limit either). For the present study, light- and strange-quark sources with much less smearing were created on ensembles **c** and **d** to better

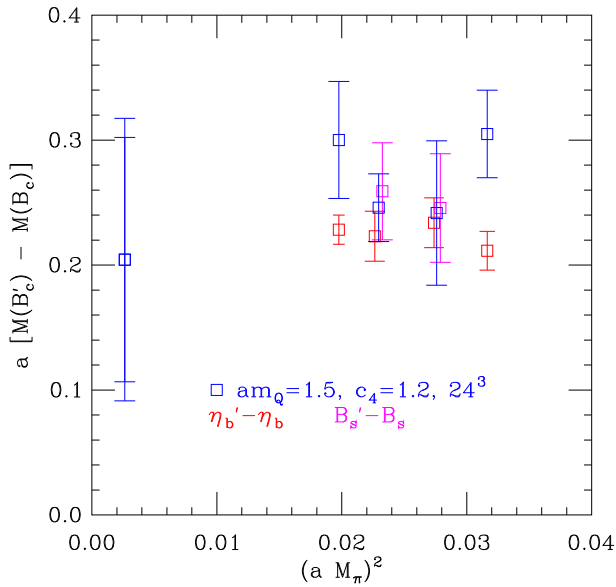


FIG. 8: Pseudoscalar $B'_c - B_c$ mass differences versus pion mass ($\eta'_b - \eta_b$ and $B'_s - B_s$ energies are also plotted for comparison).

study such states. The results for the ensemble closer to the chiral limit (c) are shown in Table IX. The results for the corresponding pseudoscalar $B'_s - B_s$ splitting appear in Fig. 8, along with the $B'_c - B_c$ and $\eta'_b - \eta_b$ differences. Clearly, many more statistics are needed here, especially to reach a more reliable chiral limit.

C. Singly heavy baryons

The naming conventions for heavy baryons may not be strictly obeyed here, especially where negative-parity

TABLE IX: Results for $B_{(s,c)}$ -meson first-excited-ground state mass splittings (in MeV) using $am_Q = 1.5$ and $c_4 = 1.2$ on ensemble c. The first error comes from the fit, the second from the scale setting (ΔM_{PS}).

splitting	$N_f = 2 + 1$ (c)
$B' - B$	670(120)(30)
$B^{*'} - B^*$	640(90)(25)
$B_0^{*'} - B_0^*$	790(160)(30)
$B_1^{*'} - B_1^*$	760(110)(30)
$B'_s - B_s$	697(100)(27)
$B_s^{*'} - B_s^*$	659(80)(25)
$B_{s0}^{*'} - B_{s0}^*$	730(110)(30)
$B_{s1}^{*'} - B_{s1}^*$	730(95)(30)
$B'_c - B_c$	661(73)(25)
$B_c^{*'} - B_c^*$	662(73)(25)
$B_{c0}^{*'} - B_{c0}^*$	630(110)(25)
$B_{c1}^{*'} - B_{c1}^*$	675(95)(26)

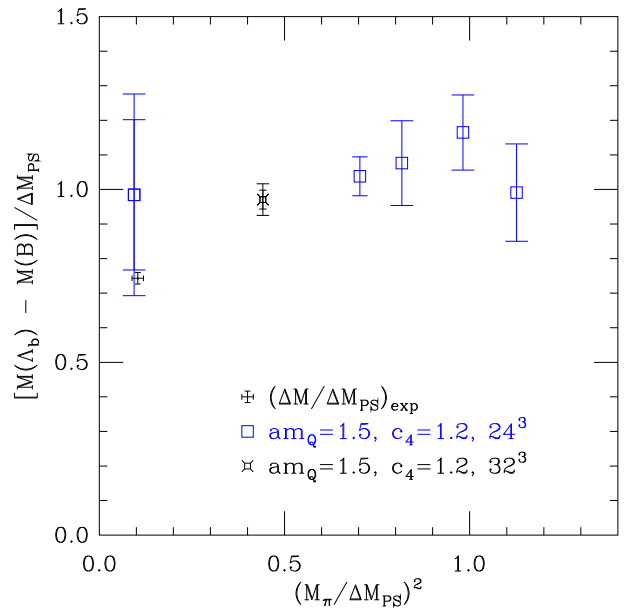


FIG. 9: $\Lambda_b - B$ mass differences versus M_π^2 .

states are concerned. Therefore, for the purpose of notational clarity, we briefly point out the quantum numbers and the corresponding names of the baryon states discussed in this subsection:

$$J^P(s_{dq}) = \frac{1}{2}^+(0) : \Lambda_b, \Xi_b$$

$$J^P(s_{dq}) = \frac{1}{2}^+(1) : \Sigma_b, \Xi_b', \Omega_b$$

$$J^P(s_{dq}) = \frac{3}{2}^+(1) : \Sigma_b^*, \Xi_b^{*'}, \Omega_b^*$$

$$J^P(s_{dq}) = \frac{1}{2}^-(0) : \Lambda_b^*, \Xi_b''$$

$$J^P(s_{dq}) = \frac{3}{2}^-(1) : \Sigma_b^{*'}, \Xi_b^{*'}, \Omega_b^{*}$$

where s_{dq} is the spin of the diquark appearing in the associated baryon interpolator (*not* that of the state).

Table X lists the results for our mass splittings among the singly heavy baryons.

Figure 9 shows the $\Lambda_b - B$ mass difference as a function of M_π^2 . The results on all lattices are high when compared to experiment, a sign that the small volumes (see Table I) may be drastically affecting our results for baryons with two light quarks. The $\Lambda_b - B$ splitting appears again in Fig. 10, along with the the analogous $\Xi_b - B_s$ splitting, but here again our lattice results are too high, 536(78) MeV (χ -extrap. $N_f = 2 + 1$), when compared to experiment (427 MeV). The $\Omega_b - B_s$ difference shows much better agreement.

Mass differences from alternative spin-flavor combinations appear in Fig. 11. Here, the (spin averaged) $\Sigma_b^{(*)} - \Lambda_b$ and $\Sigma_b^* - \Sigma_b$ splittings also show possible signs of finite-volume-induced enhancements (the dotted results are from chiral extrapolations without the heaviest pion mass, e). Other spin and multiplet splittings can be found in Table X (sometimes also with the same limited chiral extrapolation).

Figure 12 displays the mass differences between the

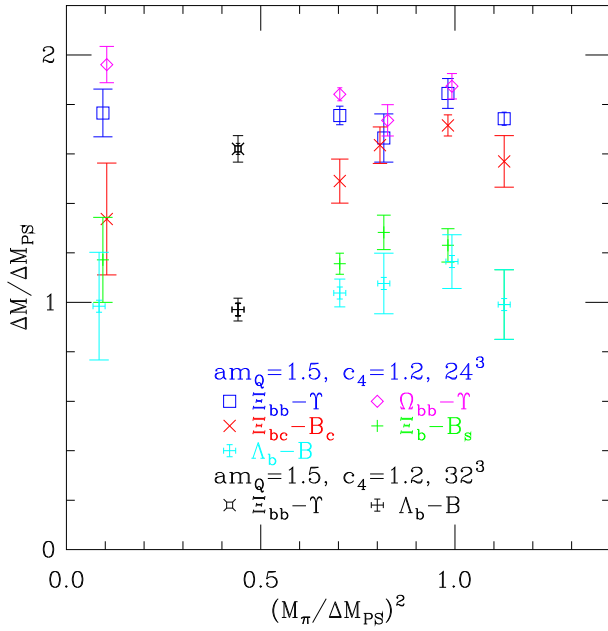


FIG. 10: $\Xi_{bb} - \Upsilon$, $\Xi_{bc} - B_c$, $\Xi_b - B_s$, and $\Lambda_b - B$ mass differences versus M_π^2 .

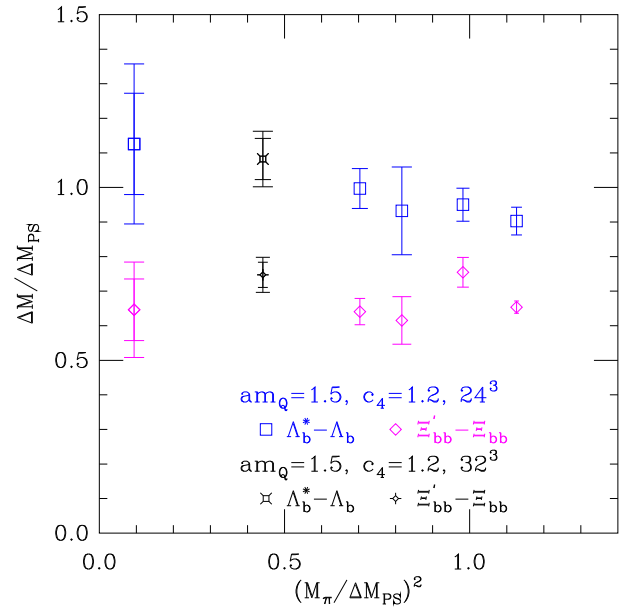


FIG. 12: Mass differences – involving the Λ_b^* and Ξ'_{bb} negative-parity states – versus M_π^2 .

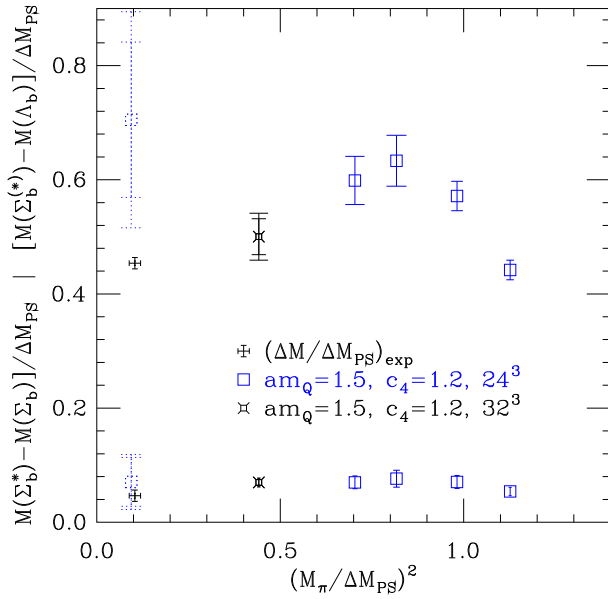


FIG. 11: $\Sigma_b^{(*)} - \Lambda_b$ and $\Sigma_b^* - \Sigma_b$ mass differences versus M_π^2 .

Λ_b and its parity partner, Λ_b^* . Again, there is a clear overestimate here; the experimental value being around 300 MeV [20]. Mass differences involving this and other negative-parity states can be found in Table X [1].

D. Doubly heavy baryons

As before, we point out the names of the states discussed in this subsection:

$$J^P(s_{dq}) = \frac{1}{2}^+(0) : \Xi_{bc}, \Omega_{bc}$$

$$J^P(s_{dq}) = \frac{1}{2}^+(1) : \Xi'_{bc}, \Omega'_{bc}, \Xi_{bb}, \Omega_{bb}$$

TABLE X: Results for bqq' (where $q, q' = u, d, s$) baryon mass splittings (in MeV) using $am_Q = 1.5$ and $c_4 = 1.2$ for the $N_f = 2 + 1$ chiral limit (χ), the $N_f = 2 + 1$ ensemble **b**, and the $N_f = 2$ ensemble **a**. The first error comes from the fit, the second from the scale setting (ΔM_{PS}). (\dagger Using only the three lightest M_π values.)

splitting	$N_f = 2 + 1$ (χ)	$N_f = 2 + 1$ (b)	$N_f = 2$ (a)
$\Lambda_b - B$	450(99)(34)	474(26)(14)	444(12)(9)
$\Xi_b - B_s$	536(78)(40)	528(20)(16)	-
$\Omega_b - B_s$	746(43)(56)	695(16)(21)	-
$\Xi_b - \Lambda_b$	231(26)(17)	87.2(8.2)(2.6)	-
$\Sigma_b^{(*)} - \Lambda_b$	322(62)(24) †	274(19)(8)	229(14)(4)
$\Xi_b - \Xi_b$	238(25)(18)	190(10)(6)	-
	154(40)(12) †		
$\Omega_b - \Xi_b$	314(34)(24)	221(12)(7)	-
$\Sigma_b^* - \Sigma_b$	32(19)(2) †	31.9(5.1)(1.0)	31.9(3.0)(0.6)
$\Xi_b^* - \Xi_b$	36.6(9.8)(2.8)	33.4(3.1)(1.0)	-
$\Omega_b^* - \Omega_b$	31.6(8.5)(2.4)	27.6(3.2)(0.8)	-
$\Lambda_b^* - \Lambda_b$	514(67)(39)	455(26)(14)	495(27)(10)
$\Xi_b'' - \Xi_b$	385(79)(29) †	398(20)(12)	-
$\Sigma_b^* - \Sigma_b^*$	142(30)(11)	183(12)(6)	274(15)(5)
$\Sigma_b^* - \Lambda_b^*$	53(14)(4)	46.1(6.4)(1.4)	36.0(4.9)(0.7)
$\Xi_b^* - \Xi_b^*$	262(36)(20)	237(15)(7)	-
$\Omega_b^* - \Omega_b^*$	308(28)(23)	249(11)(8)	-

$$\begin{aligned}
J^P(s_{dq}) &= \frac{3}{2}^+(1) : \Xi_{bc}^*, \Omega_{bc}^*, \Xi_{bb}^*, \Omega_{bb}^* \\
J^P(s_{dq}) &= \frac{1}{2}^-(0) : \Xi_{bc}^{\prime\prime}, \Omega_{bc}^{\prime\prime} \\
J^P(s_{dq}) &= \frac{1}{2}^-(1) : \Xi_{bb}^{\prime}, \Omega_{bb}^{\prime} \\
J^P(s_{dq}) &= \frac{3}{2}^-(1) : \Xi_{bc}^{\prime*}, \Omega_{bc}^{\prime*}, \Xi_{bb}^{\prime*}, \Omega_{bb}^{\prime*}
\end{aligned}$$

and any ‘‘radial’’ excitations are denoted by a (2) after the name.

Mass differences involving the bc -baryons can be found in Table XI. Those for doubly bottom baryons appear in Table XII.

Also present in the previously mentioned Fig. 10 are the results for the (yet to be observed) $\Xi_{bc} - B_c$ mass difference. Using the physical value for $M(B_c)$, we find: $M(\Xi_{bc}) = 6887(103)(46)$ MeV (χ -extrap. $N_f = 2 + 1$).

The $\Xi_{bb} - \Upsilon$ and $\Omega_{bb} - \Upsilon$ energies may also be seen in Fig. 10. With the physical value for $M(\Upsilon)$ as input, we find:

$$\begin{aligned}
M(\Xi_{bb}) &= 10201(10)(14) \text{ MeV } (N_f = 2) ; \\
M(\Xi_{bb}) &= 10267(44)(61) \text{ MeV } (\chi\text{-extrap. } N_f = 2 + 1) ; \\
M(\Omega_{bb}) &= 10356(34)(68) \text{ MeV } (\chi\text{-extrap. } N_f = 2 + 1).
\end{aligned}$$

Along with the Λ_b^* , the negative-parity Ξ_{bb}^{\prime} also appears in Fig. 12.

For more results involving spin splittings, negative-parity states, and (for the bb -baryons) first-excited states, see Tables XI and XII [1].

E. Triply heavy baryons

As before, we point out the names of the states discussed in this subsection:

$$\begin{aligned}
J^P(s_{dq}) &= \frac{1}{2}^+(1) : \Omega_{bcc}, \Omega_{bbc} \\
J^P(s_{dq}) &= \frac{3}{2}^+(1) : \Omega_{bcc}^*, \Omega_{bbc}^*, \Omega_{bbb} \\
J^P(s_{dq}) &= \frac{1}{2}^-(1) : \Omega_{bbc}^{\prime} \\
J^P(s_{dq}) &= \frac{3}{2}^-(1) : \Omega_{bcc}^{\prime*}, \Omega_{bbc}^{\prime*}
\end{aligned}$$

and any ‘‘radial’’ excitations are denoted by a (2) after the name.

Mass differences involving bcc and bbc baryons can be

TABLE XI: Results for bcq (where $q = u, d, s$) baryon mass splittings (in MeV) using $am_Q = 1.5$ and $c_4 = 1.2$ for the $N_f = 2 + 1$ chiral limit (χ) and the $N_f = 2 + 1$ ensemble **b**. The first error comes from the fit, the second from the scale setting (ΔM_{PS}).

splitting	$N_f = 2 + 1$ (χ)	$N_f = 2 + 1$ (b)
$\Xi_{bc} - B_c$	611(103)(46)	681(41)(21)
$\Omega_{bc} - \Xi_{bc}$	152(34)(11)	51(13)(2)
$\Xi_{bc}^{\prime} - \Xi_{bc}$	50(19)(4)	47.2(7.2)(1.4)
$\Omega_{bc}^{\prime} - \Omega_{bc}$	38(15)(3)	43.5(4.9)(1.3)
$\Xi_{bc}^* - \Xi_{bc}^{\prime}$	26(13)(2)	26.7(4.6)(0.8)
$\Omega_{bc}^* - \Omega_{bc}^{\prime}$	21(11)(2)	25.0(3.4)(0.8)
$\Xi_{bc}^{\prime\prime} - \Xi_{bc}^{\prime}$	290(66)(22)	314(21)(10)
$\Omega_{bc}^{\prime\prime} - \Omega_{bc}^{\prime}$	342(53)(26)	334(14)(10)
$\Xi_{bc}^{\prime*} - \Xi_{bc}^{\prime\prime}$	57(17)(4)	48.1(5.4)(1.5)
$\Omega_{bc}^{\prime*} - \Omega_{bc}^{\prime\prime}$	52(14)(4)	45.6(4.0)(1.4)

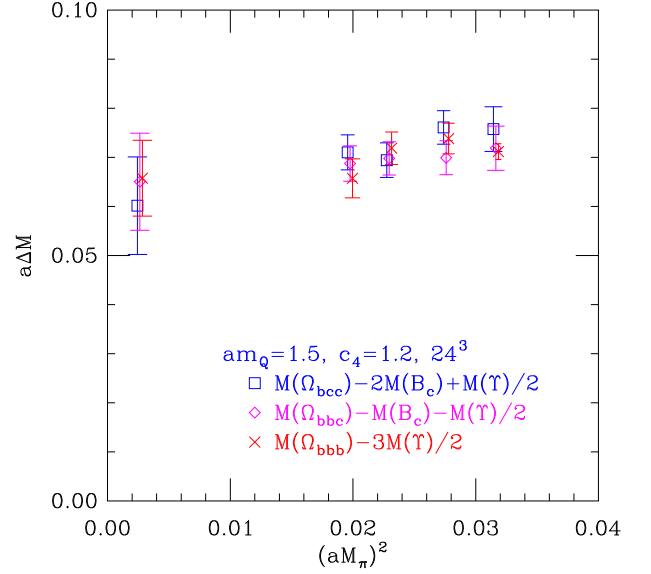


FIG. 13: Ω_{bcc} , Ω_{bbc} , and Ω_{bbb} masses versus M_π^2 .

found in Table XIII. Triply bottom results appear in Table XIV.

With the physical values for $M(B_c)$ and $M(\Upsilon)$ as input, we find:

$$\begin{aligned}
M(\Omega_{bcc}) &= 7984(27)(12) \text{ MeV } (\chi\text{-extrap. } N_f = 2 + 1) ; \\
M(\Omega_{bbc}) &= 11182(27)(13) \text{ MeV } (\chi\text{-extrap. } N_f = 2 + 1).
\end{aligned}$$

TABLE XII: Results for bbq (where $q = u, d, s$) baryon mass splittings (in MeV) using $am_Q = 1.5$ and $c_4 = 1.2$ for the $N_f = 2 + 1$ chiral limit (χ), the $N_f = 2 + 1$ ensemble **b**, and the $N_f = 2$ ensemble **a**. The first error comes from the fit, the second from the scale setting (ΔM_{PS}). (\dagger Using only the three lightest M_π values.)

splitting	$N_f = 2 + 1$ (χ)	$N_f = 2 + 1$ (b)	$N_f = 2$ (a)
$\Xi_{bb} - \Upsilon$	807(44)(61)	802(17)(24)	741(10)(14)
$\Omega_{bb} - \Upsilon$	896(34)(68)	841(12)(25)	–
$\Xi_{bb}^* - \Xi_{bb}$	49(12)(4)	33.7(4.9)(1.0)	35.1(6.5)(0.7)
	34(20)(3) \dagger		
$\Omega_{bb}^* - \Omega_{bb}$	45.1(9.5)(3.4)	32.5(3.7)(1.0)	–
	31(17)(2) \dagger		
$\Xi_{bb}^{\prime} - \Xi_{bb}$	295(41)(22)	293(17)(9)	341(17)(7)
$\Omega_{bb}^{\prime} - \Omega_{bb}$	362(44)(27)	299(19)(9)	–
$\Xi_{bb}^{\prime*} - \Xi_{bb}^{\prime}$	54(12)(4)	40.5(6.9)(1.2)	28.4(3.4)(0.6)
	40(20)(3) \dagger		
$\Omega_{bb}^{\prime*} - \Omega_{bb}^{\prime}$	50(10)(4)	37.3(5.0)(1.1)	–
	37(17)(3) \dagger		
$\Xi_{bb}(2) - \Xi_{bb}$	–	671(69)(20)	375(110)(7)
$\Xi_{bb}^*(2) - \Xi_{bb}^*$	–	591(63)(18)	387(83)(7)
$\Omega_{bb}(2) - \Omega_{bb}$	–	624(54)(19)	–
$\Omega_{bb}^*(2) - \Omega_{bb}^*$	–	564(50)(17)	–
$\Xi_{bb}^{\prime}(2) - \Xi_{bb}^{\prime}$	–	739(92)(22)	–
$\Xi_{bb}^{\prime*}(2) - \Xi_{bb}^{\prime*}$	–	793(95)(24)	–
$\Omega_{bb}^{\prime}(2) - \Omega_{bb}^{\prime}$	–	722(74)(22)	–
$\Omega_{bb}^{\prime*}(2) - \Omega_{bb}^{\prime*}$	–	711(71)(22)	–

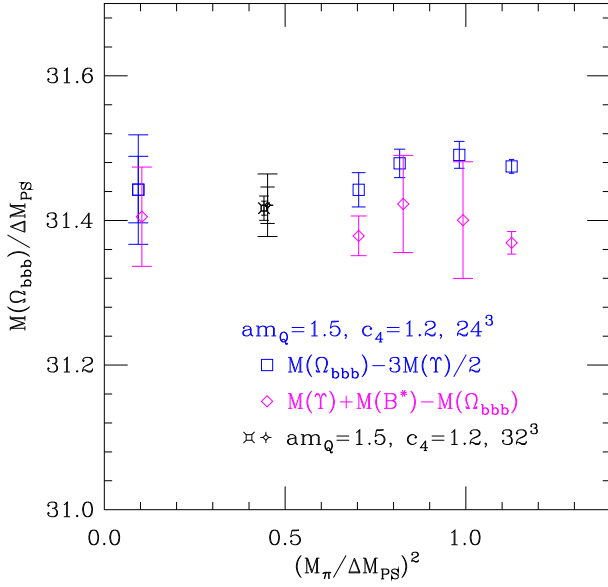


FIG. 14: Ω_{bbb} masses versus M_π^2 .

With the physical value for $M(\Upsilon)$ as input, we find:

$$M(\Omega_{bbb}) = 14357.6(4.4)(3.3) \text{ MeV } (N_f = 2) ;$$

$$M(\Omega_{bbb}) = 14369(21)(14) \text{ MeV } (\chi\text{-extrap. } N_f = 2 + 1).$$

Figure 13 shows the Ω_{bcc} , Ω_{bbc} , and Ω_{bbb} masses (referenced from an appropriate combination of $M(\Upsilon)$ and $M(B_c)$) versus the pion mass. Once the heavy-quark masses are “subtracted”, seemingly little difference remains between these triply heavy systems.

Figure 14 displays the Ω_{bbb} mass achieved via two schemes: from $E(\Omega_{bbb}) - 3E(\Upsilon)/2$ and $M(\Upsilon)$; or from $E(\Upsilon) + E(B^*) - E(\Omega_{bbb})$ and $M(\Upsilon) + M(B^*)$. The two estimates agree in the $N_f = 2 + 1$ chiral limit and on the $N_f = 2$ lattice.

For further results (e.g., spin and parity splittings) involving bcc and bbc baryons, see Table XIII. Estimates for the first-excited Ω_{bbb} appear in Table XIV.

Using (jackknifed) combinations of four correlators, we were able to compare the effect of trading one of the b quarks for a lighter one in the mesons with the same

TABLE XIII: Results for bbc and bcc baryon mass splittings (in MeV) using $am_Q = 1.5$ and $c_4 = 1.2$ for the $N_f = 2 + 1$ chiral limit (χ) and the $N_f = 2 + 1$ ensemble **b**. The first error comes from the fit, the second from the scale setting (ΔM_{PS}).

splitting	$N_f = 2 + 1$ (χ)	$N_f = 2 + 1$ (b)
$\Omega_{bcc} - 2B_c + \Upsilon/2$	164(27)(12)	185(9)(6)
$\Omega_{bbc} - B_c - \Upsilon/2$	177(27)(13)	179(9)(5)
$\Omega_{bcc}^* - \Omega_{bcc}$	28.8(5.6)(2.2)	27.2(1.8)(0.8)
$\Omega_{bbc}^* - \Omega_{bbc}$	21.8(7.0)(1.7)	26.5(2.2)(0.8)
$\Omega_{bcc}^* - \Omega_{bcc}^*$	449(41)(34)	422(15)(13)
$\Omega_{bbc}^* - \Omega_{bbc}^*$	375(74)(28)	372(26)(11)
$\Omega_{bbc}^* - \Omega_{bbc}^*$	30(12)(2)	39.6(4.1)(1.2)

effect in the baryons. These results appear in Table XV. For the first meson difference, $\Upsilon - B_c$, the spin changes from 1 to 0, but these states are much better determined (experimentally) than the corresponding η_b and B_c^* (this extra spin jump adds about 50 MeV to the first four rows). Considering the errors, there appears to be little difference between the splittings involving $\Upsilon - B_s^*$ and $\Upsilon - B^*$, but exchanging the b quark for a strange or light one appears to have a larger effect on the baryons than exchanging $b \rightarrow c$, especially when looking at baryons with fewer heavy quarks [1].

IV. DISCUSSION

We reserve this section for a brief discussion of possible sources of systematic errors affecting our results [1].

(1) Finite-volume effects:

As can be seen in Table I, all volumes are rather small when compared to the dynamical pion masses ($M_\pi L \lesssim 4$), with L ranging from 1.7–1.8 fm for the $N_f = 2 + 1$ ensembles to 2.2 fm for the $N_f = 2$ one. Obvious energy enhancements can be seen in some hadrons containing

TABLE XIV: Results for bbb baryon mass splittings (in MeV) using $am_Q = 1.5$ and $c_4 = 1.2$ for the $N_f = 2 + 1$ chiral limit (χ), the $N_f = 2 + 1$ ensemble **b**, and the $N_f = 2$ ensemble **a**. The first error comes from the fit, the second from the scale setting (ΔM_{PS}). (\ddagger Constant fit, using only the three lightest M_π values.)

splitting	$N_f = 2 + 1$ (χ)	$N_f = 2 + 1$ (b)	$N_f = 2$ (a)
$\Omega_{bbb} - 3\Upsilon/2$	179(21)(14)	172(10)(5)	167.6(4.4)(3.3)
$\Upsilon + B^* \dots$			
$-\Omega_{bbb}$	162(31)(12)	150(13)(5)	169(12)(3)
$\Omega_{bbb}(2) \dots$	211(128)(16)		
$-\Omega_{bbb}$	438(33)(33) \ddagger	411(45)(12)	480(64)(9)

TABLE XV: Comparison of meson and baryon mass splittings (in MeV) resulting from the replacement of one b quark with a lighter one. Using $am_Q = 1.5$ and $c_4 = 1.2$ for the $N_f = 2 + 1$ chiral limit (χ) and the $N_f = 2 + 1$ ensemble **b**. The first error comes from the fit, the second from the scale setting (ΔM_{PS}).

splitting	$N_f = 2 + 1$ (χ)	$N_f = 2 + 1$ (b)
$(\Upsilon - B_c) - (\Omega_{bbb} - \Omega_{bbc}^*)$	45(14)(3)	42.3(3.5)(1.3)
$(\Upsilon - B_c) - (\Omega_{bbc} - \Omega_{bcc})$	16.7(9.8)(1.3)	16.4(3.4)(0.5)
$(\Upsilon - B_c) - (\Omega_{bb} - \Omega_{bc}')$	17(32)(1)	18(12)(1)
$(\Upsilon - B_c) - (\Xi_{bb} - \Xi_{bc}')$	34(36)(3)	27(13)(1)
$(\Upsilon - B_s^*) - (\Omega_{bbb} - \Omega_{bb}^*)$	-29(20)(2)	-29.3(8.4)(0.9)
$(\Upsilon - B_s^*) - (\Omega_{bbc} - \Omega_{bc}')$	-91(27)(7)	-84.8(8.8)(2.6)
$(\Upsilon - B_s^*) - (\Omega_{bb} - \Omega_b)$	-130(50)(10)	-137(17)(4)
$(\Upsilon - B_s^*) - (\Xi_{bb} - \Xi_b')$	-171(65)(13)	-154(27)(5)
$(\Upsilon - B^*) - (\Omega_{bbb} - \Xi_{bb}^*)$	-35(20)(3)	-29.7(7.9)(0.9)
$(\Upsilon - B^*) - (\Omega_{bbc} - \Xi_{bc}')$	-112(30)(8)	-96(10)(3)
$(\Upsilon - B^*) - (\Omega_{bb} - \Xi_b')$	-137(57)(10)	-139(21)(4)
$(\Upsilon - B^*) - (\Xi_{bb} - \Sigma_b)$	-179(74)(13)	-153(33)(5)

light quarks: e.g., $\Lambda_b^{(*)}$, $\Sigma_b^{(*)}$, $\Xi_b^{\prime(*)}$, and possibly even $B^* - B$. We can only imagine how large such effects may be for higher excitations. However, there are no indications that hadrons containing strange quarks as their lightest constituents suffer from these small boxes.

(2) Different previous lattice scales; too heavy s and c quarks:

During the tuning and running stages of the present ensembles [50, 51], different scales were used than the one in the current study. The same was true during a tuning of the charm quark [54, 55]. The fact that we now use ΔM_{PS} from the bottomonia system to set the scale leads to a seemingly $\sim 10\%$ enhancement of the c and s (in the chiral limit) masses.

(3) For $N_f = 2$, too heavy b quark:

Looking at Fig. 2, one can see that on the $N_f = 2$ ensemble, $am_Q = 1.5$ is too large (by $\sim 10\%$) for the bottom quark.

(4) Different smearings; different excited-state “contamination”:

On ensembles **c** and **d**, much less smearing was chosen for the light and strange quarks in an attempt to better identify excited states. However, this may lead to different levels of contamination from excited states when considering the ratios of smeared-smeared correlators on the different ensembles leading to the $N_f = 2 + 1$ chiral limit.

(5) Relatively heavy u, d quarks; long chiral extrapolations:

For many systems considered herein, this one is not so much a systematic error, outside of the fact that it systematically causes larger errors in the chiral limit. More trouble arises from this when the system considered should cross a threshold between ensemble **b** and the chiral limit.

V. CONCLUSIONS AND OUTLOOK

We have presented the heavy-hadron spectrum arising from NRQCD-approximated b quarks and improved clover-Wilson c, s, d, u quarks on $N_f = 2$ and $2 + 1$ lattices. Singly, doubly, and triply heavy (b, c) systems were considered and results were found for spin splittings, al-

ternate parities, and in some cases, “radial” excitations. Relative mass differences between mesons and baryons resulting from the exchange of one b quark for a lighter one were presented as well. A number of systematics were pointed out (e.g., small volumes; see above), but these have not been fully quantified and the reader must use some caution with the results. Perhaps more trustworthy are the lower-lying spectra (no radial excitations) of hadrons containing only b, c , or s valence quarks. A more careful analysis of all the data generated (e.g., with $am_Q = 3.0$ or the 40^3 , $N_f = 2$ correlators) and further runs on existing 32^3 , $N_f = 2 + 1$ ensembles could uncover more about the errors incurred, and an expansion of the code [61] could lead to a study of possible $bbq\bar{q}$ states, but we must excuse ourselves from taking this project further as we have precious little free time and have found new ways in which to be wrong [69].

Acknowledgments

Light-quark propagators were generated with the use of the Chroma [53] software library. We thank our colleagues for saving the light- and strange-quark propagator files on ensembles **a, b**, and **e** [50, 54] and for making them available to the group at large. We would like to thank S. Gutzwiller and R. Schiel for help in checking that we were properly reading the light-quark propagator files and J. Najjar for providing initial plaquette results for our u_0 values. We would like to thank M. Göckeler for helpful suggestions on many topics and P. Pérez-Rubio for useful discussions involving heavy-hadron interpolators. Simulations were performed at the Uni-Regensburg Rechenzentrum and Institute for Theoretical Physics and we thank the Schäfer and Braun Chairs for continued access and the administrators for keeping the machines running smoothly. This work was supported in part by the DFG (SFB TR-55) and mostly by a patient family. Beyond the scope of this project, we would like to thank those who still deem it worthwhile to discuss physics with the unaffiliated. In the end, it must be admitted that the author has been in this place too long, rendering him a cynic [70]. Apologies for where it shows.

-
- [1] Excuse the curt presentation in places, but this is as much exodus as it is catharsis and the later-written parts of the manuscript will show it. Initially intended as part of a larger study with larger lattices, these results have been sitting around partially analyzed for a while, but they may have retained some relevance. As it always should be, use or damn what you will.
- [2] B. Aubert *et al.* [BABAR Collaboration], Phys. Rev. Lett. **101**, 071801 (2008) [Erratum-ibid. **102**, 029901 (2009)] [arXiv:0807.1086 [hep-ex]].
- [3] B. Aubert *et al.* [BABAR Collaboration], Phys. Rev. Lett. **103**, 161801 (2009) [arXiv:0903.1124 [hep-ex]].
- [4] G. Bonvicini *et al.* [CLEO Collaboration], Phys. Rev. D **81**, 031104 (2010) [arXiv:0909.5474 [hep-ex]].
- [5] S. Dobbs *et al.*, Phys. Rev. Lett. **109**, 082001 (2012) [arXiv:1204.4205 [hep-ex]].
- [6] R. Mizuk *et al.* [Belle Collaboration], Phys. Rev. Lett. **109**, 232002 (2012) [arXiv:1205.6351 [hep-ex]].
- [7] I. Adachi *et al.* [Belle Collaboration], Phys. Rev. Lett. **108**, 032001 (2012) [arXiv:1103.3419 [hep-ex]].
- [8] G. Aad *et al.* [ATLAS Collaboration], Phys. Rev. Lett. **108**, 152001 (2012) [arXiv:1112.5154 [hep-ex]].

- [9] V. M. Abazov *et al.* [D0 Collaboration], Phys. Rev. Lett. **99**, 172001 (2007).
- [10] T. Aaltonen *et al.* [CDF Collaboration], Phys. Rev. Lett. **100**, 082001 (2008) [arXiv:0710.4199 [hep-ex]].
- [11] V. M. Abazov *et al.* [D0 Collaboration], Phys. Rev. Lett. **100**, 082002 (2008).
- [12] R. Aaij *et al.* [LHCb Collaboration], arXiv:1211.5994 [hep-ex].
- [13] T. Aaltonen *et al.* [CDF Collaboration], Phys. Rev. Lett. **99**, 202001 (2007).
- [14] V. M. Abazov *et al.* [D0 Collaboration], Phys. Rev. Lett. **99**, 052001 (2007).
- [15] T. Aaltonen *et al.* [CDF Collaboration], Phys. Rev. Lett. **99**, 052002 (2007).
- [16] V. M. Abazov *et al.* [D0 Collaboration], Phys. Rev. Lett. **101**, 232002 (2008) [arXiv:0808.4142 [hep-ex]].
- [17] T. Aaltonen *et al.* [CDF Collaboration], Phys. Rev. D **80**, 072003 (2009) [arXiv:0905.3123 [hep-ex]].
- [18] R. Aaij *et al.* [LHCb Collaboration], arXiv:1302.1072 [hep-ex].
- [19] S. Chatrchyan *et al.* [CMS Collaboration], Phys. Rev. Lett. **108**, 252002 (2012) [arXiv:1204.5955 [hep-ex]].
- [20] R. Aaij *et al.* [LHCb Collaboration], Phys. Rev. Lett. **109**, 172003 (2012) [arXiv:1205.3452 [hep-ex]].
- [21] P. Palmi [for the CDF Collaboration], arXiv:1309.6269 [hep-ex].
- [22] S. Meinel, Phys. Rev. D **79**, 094501 (2009) [arXiv:0903.3224 [hep-lat]].
- [23] T. Burch *et al.*, Phys. Rev. D **81**, 034508 (2010) [arXiv:0912.2701 [hep-lat]].
- [24] S. Meinel, Phys. Rev. D **82**, 114502 (2010) [arXiv:1007.3966 [hep-lat]].
- [25] R. J. Dowdall *et al.* [HPQCD Collaboration], Phys. Rev. D **85**, 054509 (2012) [arXiv:1110.6887 [hep-lat]].
- [26] R. J. Dowdall *et al.* [HPQCD Collaboration], arXiv:1309.5797 [hep-lat].
- [27] J. O. Daldrop *et al.* [HPQCD Collaboration], Phys. Rev. Lett. **108**, 102003 (2012) [arXiv:1112.2590 [hep-lat]].
- [28] R. Lewis and R. M. Woloshyn, Phys. Rev. D **85**, 114509 (2012) [arXiv:1204.4675 [hep-lat]].
- [29] A. M. Green *et al.* [UKQCD Collaboration], Phys. Rev. D **69**, 094505 (2004) [hep-lat/0312007].
- [30] T. Burch and C. Hagen, Comput. Phys. Commun. **176**, 137 (2007) [hep-lat/0607029].
- [31] T. Burch, C. Hagen, *et al.*, Phys. Rev. D **79**, 014504 (2009) [arXiv:0809.1103 [hep-lat]]; PoS LATTICE **2008**, 110 (2008) [arXiv:0809.3923 [hep-lat]].
- [32] W. Detmold, C. -J. D. Lin, and M. Wingate, Nucl. Phys. B **818**, 17 (2009) [arXiv:0812.2583 [hep-lat]].
- [33] C. Michael *et al.* [ETM Collaboration], JHEP **1008**, 009 (2010) [arXiv:1004.4235 [hep-lat]].
- [34] E. B. Gregory *et al.*, Phys. Rev. D **83**, 014506 (2011) [arXiv:1010.3848 [hep-lat]].
- [35] C. McNeile *et al.*, Phys. Rev. D **86**, 074503 (2012) [arXiv:1207.0994 [hep-lat]].
- [36] R. J. Dowdall *et al.*, Phys. Rev. D **86**, 094510 (2012) [arXiv:1207.5149 [hep-lat]].
- [37] I. F. Allison *et al.* [HPQCD and Fermilab Lattice and UKQCD Collaborations], Phys. Rev. Lett. **94**, 172001 (2005) [hep-lat/0411027].
- [38] E. B. Gregory *et al.*, Phys. Rev. Lett. **104**, 022001 (2010) [arXiv:0909.4462 [hep-lat]].
- [39] R. Lewis and R. M. Woloshyn, Phys. Rev. D **79**, 014502 (2009) [arXiv:0806.4783 [hep-lat]].
- [40] H. Na and S. Gottlieb, PoS LATTICE **2008**, 119 (2008) [arXiv:0812.1235 [hep-lat]].
- [41] S. Meinel, Phys. Rev. D **82**, 114514 (2010) [arXiv:1008.3154 [hep-lat]].
- [42] S. Meinel, Phys. Rev. D **85**, 114510 (2012) [arXiv:1202.1312 [hep-lat]].
- [43] Z. S. Brown *et al.*, Phys. Rev. D **90**, no. 9, 094507 (2014) [arXiv:1409.0497 [hep-lat]].
- [44] M. Wurtz, R. Lewis, and R. M. Woloshyn, PoS LATTICE **2014** (2014) [arXiv:1409.7103 [hep-lat]].
- [45] C. B. Lang *et al.*, arXiv:1501.01646 [hep-lat].
- [46] R. Aaij *et al.* [LHCb Collaboration], JHEP **1410**, 88 (2014) [arXiv:1409.1408 [hep-ex]].
- [47] R. Aaij *et al.* [LHCb Collaboration], Phys. Rev. Lett. **113**, no. 24, 242002 (2014) [arXiv:1409.8568 [hep-ex]].
- [48] R. Aaij *et al.* [LHCb Collaboration], arXiv:1411.4849 [hep-ex].
- [49] B. Eakins and W. Roberts, Int. J. Mod. Phys. A **27**, 1250039 (2012) [arXiv:1201.4885 [nucl-th]]; and references therein.
- [50] G. S. Bali *et al.*, Nucl. Phys. B **866**, 1 (2013) [arXiv:1206.7034 [hep-lat]].
- [51] W. Bietenholz *et al.*, Phys. Rev. D **84**, 054509 (2011).
- [52] G. S. Bali and P. Boyle, Phys. Rev. D **59**, 114504 (1999) [hep-lat/9809180].
- [53] R. G. Edwards *et al.* [SciDAC and LHPC and UKQCD Collaborations], Nucl. Phys. Proc. Suppl. **140**, 832 (2005) [hep-lat/0409003].
- [54] G. Bali *et al.*, PoS LATTICE **2011**, 135 (2011) [arXiv:1108.6147 [hep-lat]].
- [55] G. Bali, S. Collins, and P. Pérez-Rubio, arXiv:1212.0565 [hep-lat].
- [56] P. Pérez-Rubio, arXiv:1302.5774 [hep-lat].
- [57] S. Güsken *et al.*, Phys. Lett. B **227**, 266 (1989); C. Best *et al.*, Phys. Rev. D **56**, 2743 (1997).
- [58] M. Albanese *et al.* [APE Collaboration], Phys. Lett. B **192**, 163 (1987).
- [59] G. P. Lepage *et al.*, Phys. Rev. D **46**, 4052 (1992) [hep-lat/9205007].
- [60] T. Burch and C. Ehmann, Nucl. Phys. A **797**, 33 (2007); T. Burch, “Bottomonia spectrum and scale setting on $N_f = 2$ clover-Wilson lattices,” SFB (TR55) Meeting, 23 – 24 March 2011, Regensburg; T. Burch, “Beautiful hadrons on $N_f = 2$ and $2 + 1$ improved clover-Wilson lattices,” High-Energy Theory Seminar, 11 May 2012, Regensburg.
- [61] A version of the (rather ugly) code for the NR-quark evolution and the heavy-hadron correlators has been available online at http://homepages.uni-regensburg.de/~but18772/NRQCD_HeavyLightCode.tgz (since Nov. 2014). Included therein are earlier drafts of the current paper (ca. 2013–14). Even older versions and the code itself were also previously made available on the QCDSFware website (qsdware.uni-r.de/wiki). Although I wouldn’t recommend it, feel free to use and change the code (at your own risk); if you do, please cite this paper and Ref. [60].
- [62] T. Burch and D. Toussaint [MILC Collaboration], Phys. Rev. D **68**, 094504 (2003).
- [63] G. P. Lepage and P. B. Mackenzie, Phys. Rev. D **48**, 2250 (1993).
- [64] Before they can be combined with the nonrelativistic (NR) heavy-quark propagator, the quark propagators produced by the Chroma library [53] must be rotated

from an “alternative” chiral spin-basis to the NR one: $M_{NR}^{-1} = UM^{-1}U^\dagger$, where $U = \frac{1}{\sqrt{2}}\begin{pmatrix} \sigma_y & \sigma_y \\ -\sigma_y & \sigma_y \end{pmatrix}$.

- [65] An error in the flavor projections in our code has left us without the possibility of exploring the $J = \frac{1}{2}$ states arising from the Σ_{Qi}^2 operator.
- [66] For the sake of brevity, we leave out such things as effective-mass plots, fit choices, χ^2 values, etc. The interested reader may peruse such details included in the tarball of the code [61].
- [67] J. Beringer *et al.* (Particle Data Group), Phys. Rev. D **86**, 010001 (2012).
- [68] C. E. Thomas, R. G. Edwards and J. J. Dudek, Phys. Rev. D **85**, 014507 (2012) [arXiv:1107.1930 [hep-lat]].
- [69] T. Burch and G. Torrieri [LSS Collaboration], PoS LATTICE **2013**, 055 (2014) [arXiv:1311.3333 [hep-lat]]; that, and parenting.
- [70] A. Bierce, *The Devil's Dictionary*.